ELSEVIER

Journal of Chromatography A, 704 (1995) 1–25

JOURNAL OF CHROMATOGRAPHY A

Review

Laser-induced fluorescence detection of native-fluorescent analytes in column liquid chromatography, a critical evaluation

R.J. van de Nesse, N.H. Velthorst, U.A.Th. Brinkman, C. Gooijer*

Department of Analytical Chemistry, Free University, de Boelelaan 1083, 1081 HV Amsterdam, Netherlands

First received 14 November 1994; revised manuscript received 12 January 1995; accepted 12 January 1995

Abstract

This paper critically evaluates aspects that need to be considered when applying lasers instead of conventional lamps in fluorescence detection combined with column liquid chromatography (LC). To exclude the often underestimated role of chemical derivatization reactions as far as detection limits are concerned, emphasis is on analytes showing native fluorescence. First of all basic features of both continuous wave and pulsed lasers are considered, including a quantitative treatment of saturation and photodecomposition effects. Subsequently a detailed treatment on signal-to-noise in laser induced fluorescence (LIF) is presented, the various definitions of detection limits operative in the literature are compared and flow cell constructions are considered. The paper ends with a comparison between conventional fluorescence and LIF detection in LC, an overview of published data on detection limits and a discussion on future trends.

Contents

* Corresponding author.

0021-9673/95/$29.00
SSDI 0021-9673(95)00053-4

1. Introduction

Among the many spectroscopic methods that are applied in column liquid chromatography (LC), fluorescence spectroscopy has a prominent place because of its ability to detect analytes at trace levels [1,2]. Because, in general, the fluorescence signal intensity is directly proportional with the radiant power, the sensitivity of fluorescence detection can be improved by the use of lasers instead of conventional lamps as the excitation source [3]; however, it should be kept in mind that the crucial parameter is the signal-to-noise ratio. Proper excitation wavelength selection is an aspect of primary importance. Unfortunately, most lasers provide only a number of discrete lines, while there is a lack of output in the UV part of the spectrum, especially in the deep-UV region, i.e. below 300 nm. Since there are not many relevant native-fluorescent compounds that absorb radiation in the visible range, the applicability of visible laser-induced fluorescence (LIF) is limited. This readily explains the widespread attention devoted to derivatization procedures to convert analytes into fluorescent products that can be optimally excited by means of available laser lines [4]. Although standard solutions of pure fluorophores can be quantified by LIF at extremely low concentrations, derivatization of analytes at ultra-trace levels in complex matrices gives rise to various problems and achievable limits of detection (LOD) are often several orders of magnitude higher [5]. Fortunately, recent developments in laser technology have led to the design of systems that can provide deep-UV radiation and which are (or will soon become) commercially available. It is expected therefore, that in the near future studies on LIF of native-fluorescent analytes will see a notable increase.

This paper deals with aspects that need to be considered when applying lasers instead of conventional light sources with emphasis on UV excitation. In Section 2 various laser types are discussed that can be used in LIF detection. Attention is also paid to fluorescence saturation and photochemical decomposition, phenomena that can play a role in LIF because of the high incident light powers and tightly focused laser beams. LIF detection in LC is considered in Section 3 and includes a discussion on the parameters that influence signal intensity and noise, different flow cell constructions, and a comparison between LIF and conventional fluorescence detection. Besides, the literature on LC–LIF of native-fluorescent analytes, is reviewed. Finally, in Section 4 general conclusions are drawn and future developments are outlined.

2. Basic aspects of lasers in fluorescence detection

2.1. Laser types

Since the introduction of the ruby laser in 1960 [6], several laser types have been developed and commercialized, each one with its own unique properties. The preference of an analytical spectroscopist for a particular laser system will be determined by various criteria: wavelength availability, light power, pulsed/continuous-wave (CW) operation, output stability, lifetime, required facilities, robustness, size and, last but not least, costs. Some of these aspects are mutually related. For instance, deep-UV light is provided by a very expensive argon-ion laser that requires a high power line (e.g. 360 V, 3 phase, 50 A), a large cooling facility (e.g. 20 l water min^{-1}) and much laboratory space. On the other hand, the same laser type is available as a small size air-cooled version which produces only

visible light at low power, at a price which is a fraction of that of its big brother. It is therefore difficult to make general statements about the properties of a particular laser type because different versions are commercially available; for instance, Laser Focus World Buyers Guide 27 (1992) describes more than 360 argon-ion lasers that are on the market [7]. There is one aspect, however, that applies to all lasers: increasing light power (especially in the UV region) costs money.

In this section, technical details are described of various laser types important in analytical fluorimetry. Most information is derived from Laser Focus World, a magazine that appears monthly; especially the regular contributions of J. Hecht are worthwhile [7–9].

Laser output can be continuous or pulsed. In Table 1 the most popular CW lasers applied in analytical fluorimetry are summarized. It is clear that the number of available wavelengths is limited, especially in the UV region, which is a serious shortcoming in LIF. The wavelengths produced by the argon-ion laser depend on the electrical power input. Visible laser lines arise from the emission of singly ionized argon while doubly ionized argon provides lines in the UV part of the spectrum. The latter demand high power discharges and hence large cooling requirements, facilities that are usually not available in analytical laboratories. The high-power water-cooled lasers typically come in two sizes: a 1-m "small-frame" and a 2-m "large-frame" version. At the other end is the low-power air-cooled version of the argon-ion laser which only provides 488 and 514 nm output. These wavelengths generally are too long to be used for straightforward excitation of native fluorophores; in separation sciences analytically interesting analytes are indirectly detected by labeling with a fluorescent probe which efficiently absorbs the visible laser lines [3,4]. In the past two years, the excitation possibilities of commercially available argon-ion lasers in the UV have been increased considerably. The interesting deep UV emission at 275 nm recently became available by modification of the plasma tube and mirror coatings. Further, intra-cavity frequency doubling has been commercialized so that even shorter wavelengths, i.e. 229–257 nm, are available at hundreds of milliwatts. In the past years, laser tube lifetimes have increased considerably and now range from 2000 to 10 000 h. When the laser is operated in the UV mode, its lifetime decreases

Table 1
Characteristics of CW lasers used in analytical fluorimetry

Type	Wavelength (nm)		Total output power (mW)
Argon-ion	529, 514, 502,497, 488		10–30 000[a]
	477, 473, 466, 458, 455	also air-cooled	
	364, 351, 334		5000
	306, 302, 300, 275	only water-cooled	1.5
Krypton-ion	799, 752, 677, 647, 569		
	531, 521, 483, 476, 468	also air cooled	10–5000
	415, 413, 407		
	356, 351, 338	only water-cooled	2000
Helium–cadmium	325		1–100
	354[b]		20
	442		2–150
Diode (In:Ga:Al:P)	670		10
	635		3

Data adapted from Refs. [8,10].
[a] Upper value applies to water-cooled versions.
[b] Only recenily on the market.

since much higher currents are needed. A typical feature of a deteriorating argon-ion laser is the sag of the cathode into the light beam. In our laboratory, we have extended the lifetime by turning the complete laser upside down so that gravity then acts on the other side of the cathode.

The krypton-ion laser basically uses the same construction as the argon-ion laser (mixed krypton–argon ion lasers are also available). Its output, however, is at higher wavelengths. Lasers operating on Kr^{3+} generate CW powers of 2.5 W at 242–266 nm and wavelengths as short as 219 nm, but they have not been commercialized as yet.

CW excitation in the UV part of the spectrum is provided by the compact helium–cadmium laser which is less expensive than a large-frame argon-ion laser and does not need extra facilities. A drawback is the limitation to two laser lines only, 325 and 442 nm; a second UV line at 354 nm became available recently. Lifetimes of HeCd lasers have been a problem in the past but nowadays specified lifetimes are 5000–6000 h. The most powerful commercially available version provides about 100 mW at 325 nm and 150 mW at 442 nm.

Diode lasers still typically deliver only red and infrared light; for the shortest-wavelength versions, the output is limited to a few milliwatts at wavelengths of 670 nm and 635 nm (not simultaneously provided by the same laser). For applications in analytical fluorimetry, special derivatization reagents have been developed which efficiently absorb the red light [11–14]. Low-power diode lasers are the cheapest lasers available (prices from US$ 100); they are compact and can be operated on a simple battery. The large spatial divergence of about 30° is compensated for by a lens that is incorporated in the assembly. The development towards shorter wavelengths, driven by the need for more compact information storage, has resulted in the production of diode lasers that deliver wavelengths in the green–yellow part of the spectrum, waiting to be commercialized.

Pulsed laser excitation combined with time-resolved detection can be used to discriminate between instantaneous processes such as Raman and Rayleigh scatter and the relatively long-living analyte fluorescence. Furthermore, a pulsed output is essential in non-linear processes where the efficiency of an n-photon process increases linearly with the n-th power of the irradiance (W cm^{-2}). In Table 2, the characteristics of pulsed lasers that are applied in analytical fluorimetry are summarized. Interesting aspects are the peak power, the pulse duration (important in fluorescence time-resolved detection), and the repetition rate (important for averaging pulse-to-pulse fluctuations). The nitrogen and the excimer laser usually provide a broad spatial beam of rectangular shape. As a result of the fast kinetics of the laser medium, the light amplification within one round trip is so large that in essence no mirrors are required; this behaviour is denoted as "super-radiant" emission. The laser radiation is generated by a high electrical

Table 2
Characteristics of pulsed lasers applied in analytical fluorimetry

Type	Wavelength (nm)	Average power (W)	Peak power (MW)	Pulse duration (ns)	Repetition frequency (Hz)
Excimer	308 (XeCl) 248 (KrF)	1–10	10–20	15	100–1000
Nitrogen	337	0.01–0.3	0.1–1	0.3–10	10–100
Nd:YAG[a]	1064[b]	1–10	100–200	5–10	10

Data adapted from Refs. [9,10].
[a] Flashlamp pumped.
[b] Can be frequency doubled, tripled and quadrupled to 532, 355 and 266, respectively.

discharge in a cavity filled with gas. As a result it produces large quantities of radio frequency interference (RFI) noise that is picked up by the detection system if not properly shielded. Excimer lasers are capable of producing very high average powers and are efficient for pumping dye lasers. The same laser assembly can be filled with different gases (F_2, ArF, KrCl, XeF, XeCl, KrF) so that excitation at several wavelengths is possible. Laser gas mixtures have to be replaced after, typically, one million shots. Gas cleaning equipment or gas replenishment can extend the lifetime.

The nitrogen laser provides a single line at 337 nm. It was one of the first commercially available UV lasers (1972); today it has been superseded by the excimer laser with its higher power levels and the neodymium laser with its third- and fourth-harmonic lines. The nitrogen laser has a simple construction, is easy to operate and inexpensive, and is available in very compact sizes. The pulse duration depends on the gas pressure and ranges from about 10 ns at 20 Torr (1 Torr = ca. 133 Pa) to about 300 ps at atmospheric pressure. The latter value is very suitable for time discrimination in fluorescence detection [15]. The neodymium laser, which consists of a host (often yttrium aluminium garnet, YAG) doped with Nd^{3+} ions, is a solid state laser that can be operated in the continuous mode although pulsed operation is often preferred because of the conversion efficiency in non-linear light generation; the 1064 nm output of the Nd:YAG is easily doubled, tripled, and quadrupled to 532, 355 and 266 nm, respectively. Neodymium lasers can be pumped by continuous lamps, pulsed flashlamps or the 810 nm diode laser. The latter has opened the way for compact size lasers with better output stability than the flashlamp-pumped versions.

The stability of the laser output is a critical parameter. Compared with conventional light sources lasers are, in general, more noisy which is important when the background is limiting the achievable detection limits (see Section 3). For CW lasers such as the argon- and krypton-ion lasers typical fluctuations are in the 0.5–1% range, while HeCd lasers are even less stable (1–2%). With feedback control devices the light power can be stabilized to 0.05%. Diode lasers offer extremely stable outputs and fluctuations of less than 0.005% can be reached [12]. Power reproducibility is a serious problem for pulsed lasers, especially in non-linear light generation where pulse fluctuations are further amplified. In the worst case, pulse-to-pulse fluctuations can be as high as 50% and signal averaging over a large number of pulses is needed to obtain a steady detector output. In these cases, a high repetition rate is favourable.

All the laser types mentioned above provide fixed wavelengths. Tunable wavelength selection (typically over a 50 nm range) is provided by dye lasers; because these are optically pumped, the shortest possible laser wavelength is limited by the pump source wavelength. When pumped by an argon- or krypton-ion laser, the shortest wavelength available is about 400 nm. A disadvantage of dye lasers is the photochemical decomposition of the dyes after prolonged pumping which causes a decrease in the output with time. Furthermore, the toxic nature of most dyes is an aspect of concern nowadays. Much more simple to operate are the tunable vibronic solid-state lasers such as the Ti:sapphire laser, which provides a continuous wavelength range of 660–1180 nm. Frequency doubling and tripling extends its applicability range into the UV region.

Finally, a critical survey of the available literature shows that, over the past decade, the robustness, versatility and application range of lasers have improved considerably. At the same time, prices have gone down. As a result, lasers have become a much more popular tool for analytical studies and application-orientated work.

2.2. Influence of excitation power on fluorescence intensity

The sensitivity of fluorescence detection can be increased by the high light intensity that lasers provide. The number of photons emitted per second by an illuminated sample that arrives at

the photocathode of a photomultiplier is given by:

$$n_f = 2.3\,\epsilon_\lambda\,[\text{analyte}]\,L\,\phi_f\,P_{ex}\,C \quad (1)$$

where ϵ_λ is the molar absorptivity ($l\,mol^{-1}\,cm^{-1}$), [analyte] the concentration of fluorophore ($mol\,l^{-1}$), L is the optical path length (cm), ϕ_f the fluorescence quantum yield, P_{ex} the incident radiant power (photons s^{-1}) and C the collection efficiency of the optical system of the detector. Eq. 1 holds if inner filter effects play no role so that the incident power, P_{ex}, is constant along the light path. The sensitivity of fluorescence detection can not be improved indefinitely by increasing laser power. At high incident radiation ground state depletion may occur and the fluorescence signal will no longer be proportional with the excitation power. Furthermore, the effect of photodestruction, which causes a decrease of the fluorescence signal with time, shows up more strongly at higher powers.

For CW lasers, the fluorescence intensity under saturation conditions can be calculated by assuming a steady state between the various molecular processes depicted in the kinetic scheme of Fig. 1. The number of photons emitted per second from an irradiated volume is:

$$n_f = k_f\,[S_1]\,V = \frac{k_f\,k_{ex}\,[\text{analyte}_{tot}]}{k_{ex} + k_f + k_{nr} + k_{ex}\,k_{isc}/k_T}\,V \quad (2)$$

where k_f is the fluorescence rate constant, k_{nr} is the sum of all non-radiative processes that depopulate the S_1 state (internal conversion, intersystem crossing and bimolecular quenching: $k_{ic} + k_{isc} + k_q[Q]$), k_T is the total decay rate constant for the T_1 state and V is the illuminated volume (cm^3); [analyte$_{tot}$] (molecules cm^{-3}) represents the total population of molecules in the three electronic states involved ($[S_0] + [S_1] + [T_1]$). The rate constant of excitation, k_{ex}, is determined by the light intensity and the molecular tendency for light absorption according to:

$$k_{ex} = \sigma_\lambda\,I = \frac{2300\,\epsilon_\lambda\,I}{N_A} = 3.8 \cdot 10^{-21}\,\epsilon_\lambda\,I \quad (3)$$

with σ_λ the absorption cross section (cm^2 molecule^{-1}), I the incident light intensity (photons $s^{-1}\,cm^{-2}$), ϵ_λ the molar absorptivity ($l\,mol^{-1}\,cm^{-1}$), and N_A Avogadro's number. At low irradiances (photons $s^{-1}\,cm^{-2}$), i.e. k_{ex} or $(k_{ex}\,k_{isc}/k_T) < (k_f + k_{nr})$, Eq. 2 reduces to the simpler Eq. 1. High irradiances occur when tight focusing is applied and/or with pulsed lasers as excitation source.

As an example, Table 3 shows calculated data which illustrate the effect of focusing, using molecular parameters that are typical for aromatic hydrocarbons. The number of photons that is emitted by one molecule irradiated during one second is calculated with Eq. 2 using an analyte concentration of one molecule per irradiated sample volume. The fluorescence signal from this volume is expressed by taking the illuminated area into account (photons mm^2 molecule^{-1} s^{-1}). For simplicity it was assumed that the light is uniformly distributed. The percent population distribution of the excited states is given by:

$$\%S_1 = \frac{k_{ex}}{k_{ex} + k_f + k_{nr} + k_{ex}\,k_{isc}/k_T} \times 100\% \quad (4)$$

$$\%S_0 = 100\% - \%S_1 \times (1 + k_{isc}/k_T) \quad (5)$$

$$\%T_1 = \%S_1 \times k_{isc}/k_T \quad (6)$$

The data on CW laser excitation show that with the numerical values used, saturation will occur for spot diameters smaller than 100 μm, dimensions that are typical for flow cells used in open-tubular LC and capillary electrophoresis

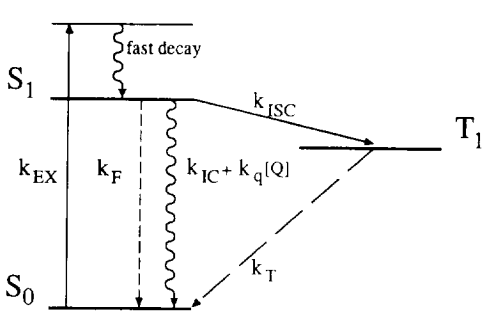

Fig. 1. Designation of intramolecular processes between singlet (S_0 and S_1) and triplet (T_1) states used in the kinetic equations in the text.

Table 3
Effect of focusing of CW and pulsed laser light on the population distribution of the three electronic states involved and the fluorescence intensity

Spot diameter (μm)	Continuous wave					
	k_{ex} (s^{-1})	$\%S_0$	$\%S_1$	$\%T_1$	Emitted photons (molecule^{-1} s^{-1})	Fluorescence intensity (photons mm^2 molecule^{-1} s^{-1})
1000	$9.6 \cdot 10^3$	99.90	0.009	0.09	$4.8 \cdot 10^3$	4800
100	$9.6 \cdot 10^5$	90.45	0.87	8.68	$4.4 \cdot 10^5$	4400
10	$9.6 \cdot 10^7$	8.65	8.30	83.05	$4.2 \cdot 10^6$	420
	100 Hz pulsed					
	k_{ex}^a (s^{-1})	$\%S_0^b$	$\%S_1^b$	$\%T_1^b$	Emitted photons (molecule^{-1} s^{-1})	Fluorescence intensity (photons mm^2 molecule^{-1} s^{-1})
1000	$9.6 \cdot 10^9$	0.85	89.88	9.27	92	92
100	$9.6 \cdot 10^{11}$	0.85	89.88	9.27	92	0.92
10	$9.6 \cdot 10^{13}$	0.85	89.88	9.27	92	0.0092

Excitation power ($\lambda_{ex} = 500$ nm): CW, 1 W; 100 Hz pulsed, 1 $W_{average}$, 1 MW_{peak} in rectangular 10 ns pulses. Molecular parameters: $\epsilon = 10\,000$ l mol^{-1} cm^{-1}, $\phi_f = 0.5$, $k_f = 5 \cdot 10^7$ s^{-1}, $k_{nr} = 5 \cdot 10^7$ s^{-1}, $k_{isc} = 10^7$ s^{-1}, $k_T = 10^6$ s^{-1}.
[a] In the pulse.
[b] Calculated at $t = 10$ ns.

(CE) (see Table 6). Obviously, for these micro-separation systems, excitation with a high-power laser is not efficient [16]. When the spot diameter is reduced from 1000 to 10 μm, which causes a 10 000-fold increase of the irradiance, the number of fluorescence photons emitted per molecule increases no more than 900-fold. The total fluorescence signal is determined by the number of molecules probed: as the illuminated area is 10 000-fold smaller, the net effect of saturation is an 11-fold lower fluorescence intensity (assuming the same optical path lengths). It should be noted that for this particular set of parameters, the main bottleneck in the saturation process is the relatively large k_{isc}/k_T ratio: at high irradiances a large part of the molecules is trapped in the triplet state.

Pulsed lasers provide about the same average power as CW lasers, but the light is typically concentrated in 10–100 pulses s^{-1} of about 10 ns. Consequently, the light power during the pulse is much higher and fluorescence saturation will occur more easily than with continuous excitation [17,18]. Because the pulse duration is on the same time scale as the inverse molecular rate constants denoted above, for pulsed laser-induced fluorescence the kinetics of fluorescence intensity can not be treated assuming steady-state conditions. For simplified temporal pulse profiles, the kinetic equations can be solved analytically although they are rather complicated [19]. An alternative approach is to use a numerical treatment of the problem [20]. The laser pulse is divided into small time intervals and the distribution between the molecular states at a particular time interval, t, is calculated by taking the values of the previous interval, $t - \Delta t$, as starting set. To illustrate the calculation procedure, which is simplified in this particular example by taking into account only two pathways, i.e. absorption and fluorescence, the number of molecules in the excited state at time t is given by:

$$[S_1]_t = [S_1]_{t-\Delta t} + k_{ex}[S_0]_t \Delta t - k_f[S_1]_t \Delta t \quad (7)$$

The total number of analyte molecules is constant, that is:

$$[S_0]_t = [\text{analyte}_{tot}] - [S_1]_t \quad (8)$$

By substituting Eq. 8 into Eq. 7 the problem can be solved. Every time increment is evaluated in a computer programme loop. With a more advanced programme, which takes into account the triplet state, the population distribution and the number of emitted photons of Table 3 were also calculated for a 1-W 100 Hz pulsed laser providing temporal rectangular 10 ns pulses. The result of these calculations shows that the number of emitted photons per molecule is independent of the irradiance, due to the fact that even for the largest spot size, i.e., 1000 μm diameter, the ground state is almost completely depleted. Fig. 2 gives the corresponding population distribution of the S_1 and T_1 states as a function of time. Initially, nearly all molecules are excited in S_1. Subsequently, inter-system crossing causes T_1 to be populated; after the pulse both excited states depopulate, S_1 much more rapidly than T_1. The number of fluorescence photons emitted per molecule per pulse is only 0.92 (Table 3). When taking into account the pulse frequency of 100 Hz it is evident that, for the present parameters, pulsed laser excitation yields low fluorescence intensity compared with CW excitation (92 vs. 4800 photons molecule^{-1} s^{-1} for 1000 μm beam diameter). When saturation conditions are met, further focusing of the laser beam will result in a decrease of the total fluorescence

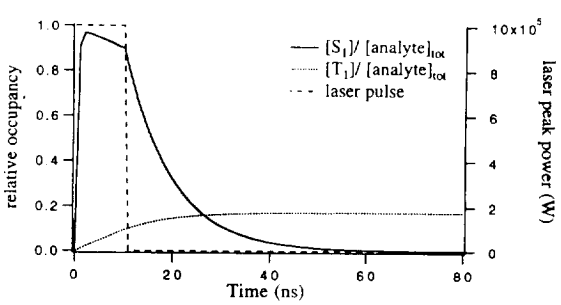

Fig. 2. Relative occupancy of the S_1 and T_1 states of a molecule (for intramolecular rate constants see Table 3) as a function of time upon excitation with a rectangular temporal 10 ns laser pulse having a peak power of $1 \cdot 10^6$ W and focused to a spot diameter of 1000 μm. Note that molecules excited to the triplet state will not decay to the ground state within the pulse duration; this decay typically takes 10 μs.

intensity since the number of probed molecules will become less. In fact fluorescence saturation with the 100 Hz pulsed laser occurs already at average irradiances as low as 1 mW mm^{-2} (occupancy of S_0: 94%). This value is in line with data in literature on fluorescence saturation with a 100 Hz excimer laser [17]. The above calculations indicate that the high light power of pulsed lasers can not be fully exploited in LIF detection. Of course the net effect of saturation on analyte detectability is also determined by the dependence of the background signal on the irradiance. For scatter processes, the background signal is linearly dependent on the applied laser power, which means that under saturation conditions, higher irradiances will lead to less favourable limits of detection. On the other hand, when the background is merely due to luminescence of impurities, saturation of the background signal may also occur and the LODs may occasionally improve.

Another point that should be considered is the photodegradation of analyte molecules upon prolonged laser excitation. Photodegradation may result from spontaneous decomposition of excited singlet or triplet states, or from a bimolecular reaction of these states with oxygen. When photodecomposition occurs from S_1, the loss of fluorophores can be written as:

$$-\frac{d[\text{analyte}]}{dt} = k_d[S_1]_t \quad (9)$$

where k_d is the pseudo first order decomposition rate constant. Since photodecomposition is a relatively slow process, steady-state conditions can be assumed for the faster molecular processes and integration of Eq. 9 yields:

$$\frac{[\text{analyte}]_t}{[\text{analyte}]_{t=0}} = \exp\left(\frac{-t\,k_d\,k_{ex}}{k_{ex} + k_f + k_{nr} + k_{ex}\,k_{isc}/k_T}\right) \quad (10)$$

Although the quantum yield of photodestruction is in general much smaller than the fluorescence quantum yield (values of 10^{-5} are reported [21,22]), its effect on the fluorescence intensity can be considerable because a molecule proceeds through many round trips during the transit

time. For instance, when a non-flowing sample containing molecules with photophysical parameters as in Table 3 and a photodestruction quantum yield of $5 \cdot 10^{-5}$ is illuminated at an irradiance of 1 W mm^{-2}, it can be calculated with Eq. 10 that 50% of the molecules will be destroyed after 1.4 s of irradiation time. In an LC system molecules are only exposed to laser light during the time interval Δt that is needed to cross the laser beam, which is often much less than 1 s. The number of fluorescent photons emitted per molecule traversing the illuminated volume, $n_{f,molecule}$, can be calculated by combining Eqs. 10 and 2 and integrating over time:

$$n_{f,molecule} = \frac{\phi_f}{\phi_d}\left[1 - \exp\left(\frac{-\Delta t\, k_d\, k_{ex}}{k_{ex} + k_f + k_{nr} + k_{ex}\, k_{isc}/k_T}\right)\right] \quad (11)$$

where ϕ_f and ϕ_d are the quantum yields of fluorescence and photodestruction, respectively. In an LC system there is a continuous transport of new of molecules in the light beam and molecules.

The impact of photodestruction for a CW and a pulsed laser is shown in Table 4, assuming a photodestruction quantum yield of $5 \cdot 10^{-5}$. Using the same molecular parameters as in Table 3, the number of fluorescent photons emitted per second in a probed area is calculated that arises from the illumination by 1-W laser light of a flowing sample having a linear velocity of 1 cm s^{-1}; the latter value corresponds to a typical flow-rate of 0.6 l min^{-1} in conventional-size LC with a 2–3 mm I.D. column. For simplicity the laser light is assumed to be uniformly distributed over a square-shaped spot. In order to distinguish between photodestruction and saturation effects, data calculated in the absence of photodestruction are also presented ($\phi_d = 0$). The fluorescence intensity is calculated by taking the illuminated area into account (photons mm^2 molecule^{-1} s^{-1}). The data of Table 4 indicate that with CW excitation the effect of photodestruction on analyte detectability is only marginal compared to saturation. The deviating percentage of destroyed molecules at the 10 μm spot size is caused by the fact that in this situation, most molecules are in T_1 from which, in this particular case, no photodecomposition was assumed to take place. Photodestruction and saturation can be distinguished experimentally by changing the flow-rate and hence, the transit time. From the dependence of the fluorescence intensity on the flow-rate, the quantum yield of photodestruction can be calculated [23]. The results in Table 4 apply for the standard geome-

Table 4
Effect of focusing and photodestruction on fluorescence intensity and percent molecules destroyed

Spot diameter (μm)	Continuous wave			100 Hz pulsed		
	Fluorescence intensity (photons mm^2 (molecule^{-1} s^{-1})		Molecules destroyed (%)	Fluorescence intensity (photons mm^2 molecule^{-1} s^{-1})		Molecules destroyed (%)
	$\phi_d = 0$	$\phi_d = 5 \cdot 10^{-5}$		$\phi_d = 0$	$\phi_d = 5 \cdot 10^{-5}$	
1000	4790	4680	5	92	92	0
500	4780	4550	9	23	23	0
250	4720	4290	17	5.8	5.8	0
100	4340	3510	35	0.92	0.92	0
50	3370	2440	49	0.23	0.23	0
25	1790	1270	51	0.058	0.058	0
10	420	340	34	0.0092	0.0092	0.01

Exposure of a streaming sample to 1 W 500 nm light from a CW laser and a 100 Hz laser providing 10 ns pulses. Linear flow-rate, 1 cm s^{-1}; molecular parameters are the same as in Table 3.

try with excitation perpendicular to the flow direction. In flow-cell assemblies where excitation light is pointed in the flow direction to achieve an increase of the optical path length, transit times are much longer and significant photodestruction has been reported [24,25].

With the pulsed laser, the number of emitted photons per molecule is constant since the ground state is almost completely depleted during the laser pulse. Because the number of probed molecules is directly proportional with the illuminated area a net decrease of signal intensity is observed. Photodestruction does hardly occur with the pulsed laser because the molecule proceeds through only 1.8 round trips during a pulse which is not much in view of the photodestruction quantum yield. It should be mentioned that the present model does not include photochemical pathways involving the triplet state or multi-photon processes, although especially the latter may be operative upon pulsed-laser irradiation.

3. LIF as detection method for LC

On account of the linear power dependence of fluorescence intensity (see Eq. 1), the introduction of lasers as excitation source for fluorescence detection in LC seems obvious. The high power of the light beam which, moreover, can be focused easily and efficiently, provides a much higher radiation yield in the flow cell than conventional light sources do. From an analytical point of view, two aspects are important to consider here; applicability to a wide range of analytes and detectability at trace levels. As regards the former aspect, new developments in laser technology keep increasing the freedom of choice of excitation wavelength, especially in the interesting UV region. The other aspect is a challenge for the analytical chemist: how does one "extract" as many fluorescent photons as possible from a sample while suppressing the background to a minimum. First, we consider important items such as the origin of background signals, signal-to-noise ratio (S/N) and the definition of the detection limit. Subsequently, applications of LIF in LC will be discussed, with emphasis on native-fluorescent analytes.

3.1. Signal-to-noise considerations

3.1.1. Background

The background is an important parameter in trace-level analysis. In general, in fluorescence detection it is the result of various contributions; the main ones are discussed below.

3.1.1.1. Laser light reflected and refracted at the flow cell

In principle, this light can readily be blocked by optical filters; however, because the laser light can be very intense, the optical density of the filter should be extremely high (transmittance $< 10^{-4}$). Care should be taken to use filters that exhibit no luminescence on exposure to the laser light, as is often encountered when glass filters are applied. Chemical filters, which consist of a solution of an inorganic salt in distilled water, usually do not show unwanted luminescence. Stray light especially occurs at the boundaries of the flow cell walls and various cell configurations and assemblies have been tested to decrease its importance (see Section 3.2).

Although lasers provide optically pure lines, the output may contain low intensity light of non-selected wavelengths which arises from spontaneous emission. If these non-lasing lines are not blocked before they enter the flow cell and if the emission filter of the detector is transparent for the corresponding wavelengths, they may seriously contribute to the background.

3.1.1.2. Rayleigh and Raman scatter from the LC eluent

The intensity of both types of scatter varies inversely proportional with the fourth power of the excitation wavelength. This means that the scatter efficiency of the 257-nm line of the frequency-doubled argon-ion laser is 16-fold higher than that of the 514-nm line. Compared to refracted and reflected laser light, the contribution of Rayleigh scatter light is only of minor importance. Raman scatter, on the other hand, causes serious problems in detection because the

Raman spectrum can overlap with fluorescence spectrum of the analyte. The spectral width of a Raman line is at least as large as the spectral band width of the excitation source. The cross section of a Raman transition is typically on the order of 10^{-28} cm^2, which is about 12 orders of magnitude smaller than a typical absorption cross section of about 10^{-16} cm^2 (corresponding with a molar absorptivity ϵ of 26 000 $l\,cm^{-1}\,mol^{-1}$). Assuming parameters that are typical in fluorescence detection, such as an analyte with a 20% quantum yield present in 20 M solvent, and a 10-nm spectral detection window that selects the fluorescence light from the 100-nm broad emission spectrum, it can be calculated that Raman background signals are comparable to analyte fluorescence signals at an analyte concentration in the flow cell of 10^{-9} *M*.

Unlike fluorescence, Raman scatter is anisotropically distributed so that the signal-to-noise ratio (S/N), in principle, can be improved with polarized laser light and a proper choice of the angle of collection and emission polarizers [26].

Fig. 3 shows the Raman spectra of the three solvents mostly used in reversed-phase LC.

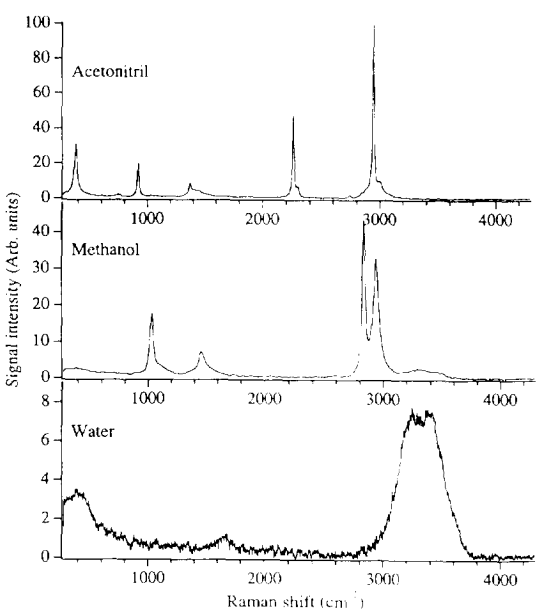

Fig. 3. Raman spectrum of solvents often used in reversed-phase LC.

When the Raman spectrum overlaps with the analyte fluorescence, interference filters can be used to select the analyte fluorescence in the spectral gaps between the baseline-resolved Raman peaks. It is often more convenient to select the optical region at the long-wavelength side of the highest Raman frequency with simple optical cut-off filters. Since the Raman bands shift with the excitation wavelength, short laser wavelengths can be used to prevent Raman interferences. In reversed-phase LC, the longest wavelength of the Raman spectrum results from the relatively broad OH-stretch band of water and methanol, which ranges from about 3000 to 3700 cm^{-1}. In Fig. 4 the minimal wavelength distance between excitation and emission settings is shown that is needed to prevent detection of this Raman scatter light. At long excitation wavelengths, such as the 670 nm light provided by diode lasers, it is only practicable to detect analyte fluorescence between the eluent Raman peaks since the OH stretch band extends to a wavelength region where common photomultipliers display no or little sensitivity.

Stray light and Rayleigh and Raman scatter are instantaneous processes, which allow time discrimination in favour of the slower fluorescence when pulsed laser sources are used. Unfortunately, this is much easier in frozen than in fluid solutions, since under the former conditions fluorescence lifetimes are usually significantly larger. In LC, lifetimes are often less than 10 ns,

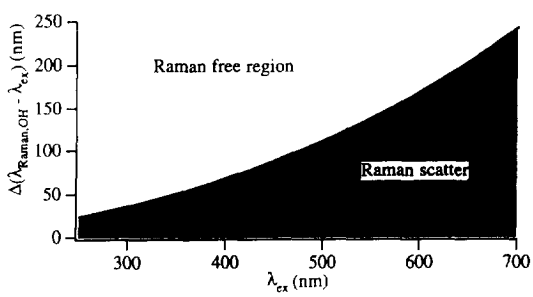

Fig. 4. Wavelength distance between excitation wavelength and the Raman OH-stretch vibration of water at 3700 cm^{-1} as a function of excitation wavelength. When analyte fluorescence is recorded at larger wavelength distances, Raman signals do not contribute to the observed background.

which means that only sharp laser pulses of about 1 ns allow effective discrimination.

3.1.1.3. Background luminescence

Background luminescence signals that are constant during a chromatographic run arise from the entire flow cell assembly —i.e. cuvette walls, flow-cell holder walls, collecting optics, optical filters and fibers— induced directly by laser light or indirectly by stray light and, last but not least, eluent impurities [27,28]. Luminescence from optical components can be decreased by using high spectral quality material; especially for the flow cell, which is exposed to the highest irradiance, Suprasil I quality quartz material is recommended. Eluent solvents that seem optically pure in conventional fluorimetry often need further purification such as distillation when LIF detection is used. Impurities that are present in the injected sample from the matrix and/or derivatization procedures, cause a varying background signal during chromatography which frequently —and unfortunately— plays the dominant role. In this case, clean-up procedures and optimization of the chromatographic system by choosing the proper column material and eluent conditions are necessary to decrease the effect of coeluting substances. In general, background luminescence is more intense at short wavelengths because the number of impurities that is excited increases.

The relative importance of the three types of background considered above strongly depends on the particular excitation and emission settings. When excitation is performed with, e.g., diode lasers at 670 nm, the analyte emission is measured in the spectral regions between the Raman peaks and the background is mainly determined by Raman scatter when native-fluorescent compounds are measured, despite its λ^{-4} intensity dependence; impurity fluorescence form matrix constituents often is negligible in this wavelength region [29]. On the other hand, excitation at 257 nm using a frequency-doubled argon-ion laser will cause relatively high backgrounds from luminescent impurities; the influence of intense Raman scatter can be reduced by recording fluorescence at longer wavelengths, i.e. above 290 nm [30].

3.1.2. Noise

The lowest signal intensity that can be detected is determined by the fluctuations of the background signal, denoted as noise. Usually, the assumption is made that the noise is normally distributed around a mean value according to a Gaussian function. However, noise may also include fluctuations which do not obey a regular distribution law, such as those produced by spikes on the line voltage or other disturbances from electrical equipment in the vicinity [31]. The noise intensity can be expressed as the standard deviation of the background signal measurements, denoted as the root-mean-square (RMS) noise, or the peak-to-peak value which is the difference between the minimum and maximum background signal. In Fig. 5 a typical time recording of a background signal is shown using an integration time of 1 s. For a normal distribution, 99.7% of all data points fall within ± 2.5 standard deviation ($\pm 2.5\ \sigma$) of the mean; in other words, for a chromatogram consisting of

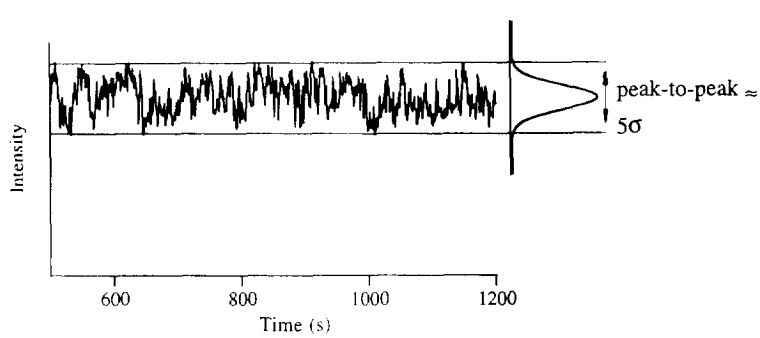

Fig. 5. Background recording showing the noise criterion.

1000 data points, only 3 points will be outside this range. It is therefore justified to estimate the RMS noise to be approximately 20% of the peak-to-peak value of a sufficiently long baseline recording.

Shot noise and flicker noise are the two major noise sources encountered in fluorescence detection. Shot noise is due to the random behaviour of light and matter. For instance, photons from a light source which impinge on a surface (e.g. the cathode of a photomultiplier) arrive randomly in time because they are not evenly spaced. The same random behaviour is observed for the thermal excitation of electrons from the photomultiplier cathode which leads to dark current. Shot noise follows the Poisson probability distribution function which means that the standard deviation or RMS noise of the number of events (e.g. photons or electrons) counted over time t, σ_{sn}, equals the square root of the number of events, n:

$$\sigma_{sn} = \sqrt{n} \tag{12}$$

Since the shot noise from background light (bl) and dark current (dc) photoelectrons are non-correlated, the total shot noise is given by [32]:

$$\sigma_{sn} = \sqrt{(\sigma_{bl})^2 + (\sigma_{dc})^2} \tag{13}$$

In analog signal processing, the relative standard deviation (R.S.D.) of the distribution of photoelectrons emitted from the cathode is preserved in the electrical signal output of the readout device since both signal and noise are multiplied by the same linear factors. After signal processing the output of the readout device is usually expressed in volts and registered by a recorder. When, during t seconds, n_{bl} background light photons arrive at the cathode with quantum efficiency θ and the dark current is generated by thermal excitation of n_{dc} photons, the background signal, $B_{total,volt}$, and the shot noise, $\sigma_{sn,volt}$, after processing by the readout device are:

$$B_{total,volt} = B_{bl,volt} + B_{dc,volt} = g(\theta n_{bl} + n_{dc}) \tag{14}$$

and

$$\sigma_{sn,volt} = g\sqrt{\theta n_{bl} + n_{dc}} = \sqrt{gB_{bl,volt} + gB_{dc,volt}} \tag{15}$$

respectively, where g(V) is the overall conversion factor that includes the gain of the photomultiplier, the signal processing and readout step.

Flicker noise is due to variations in the intensity of the light source or spatial vibrations in the experimental set-up. The magnitude of this type of noise, denoted as flicker noise, σ_{fn}, is directly proportional with the background signal. The flicker factor, ξ, is the experimentally observed R.S.D. of these instabilities for a given time constant or integration time, i.e.:

$$\sigma_{fn,volt} = \xi B_{bl,volt} \tag{16}$$

The total noise from the background light therefore is:

$$\sigma_{total,volt} = \sqrt{gB_{bl,volt} + gB_{dc,volt} + (\xi B_{bl,volt})^2} \tag{17}$$

The relative importance of shot and flicker noise is demonstrated in Fig. 6 where the peak-to-peak noise ($5\sigma_{total,volt}$) is plotted against the total background signal, B_{total}, assuming a dark current of 10 mV and $g = 10^{-6}$ V. The flicker factors (0.5% and 2.5%) are expressed as the percentage peak-to-peak noise of the background, so that $\xi_{p-p} = 5\xi \cdot 100\%$. From the figure

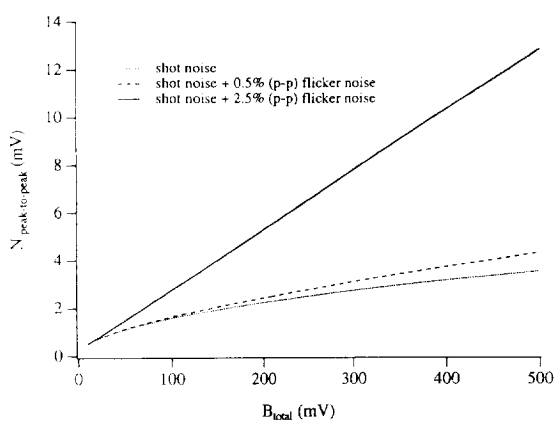

Fig. 6. Plot of peak-to-peak noise as a function of total background signal showing the effect of flicker noise.

it is noted that at low backgrounds ($B_{total,volt} <$ 20 mV), the dark current noise ($N_{p-p} = 0.5$ mV) dominates. In this situation it is worth cooling the photomultiplier tube to decrease the release of thermally induced photoelectrons from the cathode. The relative contribution of the dark current compared to the other noise sources decreases rapidly with increasing background, especially if high flicker factors are encountered. For stable light sources ($\xi_{p-p} \leq 0.5\%$), shot noise is dominant over a wide background signal range and S/N can be improved by applying higher light powers because background as well as analyte signals increase linearly with the incident radiation in fluorescence detection. Under these conditions, the potential of laser excitation is obvious. A xenon-arc lamp in a conventional detector typically provides 100 μW focused in the flow cell, so that the use of a 1-W laser would yield 10 000-fold higher background and analyte signals and, under shot noise limited conditions, 100-fold better S/N ratios. In practice a gain of two decades is not readily achieved. Especially, when unstable light sources such as pulsed lasers and the non-stabilized HeCd laser are used, flicker noise already becomes dominant at low background values and noise increases linearly with the background. In this situation substituting a laser for a lamp and/or increasing the laser power will hardly or not improve S/N values.

Generally speaking, lasers provide a less stable light output than conventional sources and flicker noise limits analyte detectability. In order to decrease flicker noise, at the excitation side lasers can be stabilized by a feedback device consisting of a photodiode that monitors the intensity variations and is coupled to a light intensity regulator, for instance an electro-optical polarizer; on the detection side, fluctuations can be corrected for by ratioing the sample signal with the reference signal of, e.g., the above photodiode [30,33].

3.1.3. Detection limit

Although attempts have been made to introduce a standardized chromatographic limit of detection [31,34,35], a variety of definitions is used throughout literature. LODs are expressed in terms of injected concentration, C_{inj} (mol l^{-1}), injected mass, M_{inj} (kg), or the peak concentration present in the detector, C_{det} (mol l^{-1}). In the last instance, the dilution in the chromatographic system is taken into account. The three parameters are related as:

$$C_{det} = \frac{C_{inj} \cdot V_{inj}}{\sigma_v \sqrt{2\pi}} = \frac{M_{inj}}{\sigma_v \sqrt{2\pi}} \tag{18}$$

where σ_v is the (volume) standard deviation of the (Gaussian) chromatographic peak. The LOD is usually defined as the signal that is 2- or 3-fold higher than the noise. Unfortunately, some authors use the RMS noise whereas others take the peak-to-peak value. Furthermore, the signal and noise intensities depend on the detector integration or RC times, t_{det}; that is S/N increases linearly with $\sqrt{t_{det}}$.

As an example, in Table 5 two LODs are calculated using the same chromatographic system and detector, but different LOD definitions, noise criterions and time constants. The 250-fold difference in LOD that is found clearly shows the importance of reporting the experimental and mathematical conditions used in the determination and calculation of one's LOD values.

3.2. Detector flow cell constructions

Since the first application of LIF as a detection method in LC by Diebold and Zare [36], special attention has been paid to the optimization of the flow cell assembly, which is a critical part in the detection system. Because in LIF the incident light power is much higher than with conventional fluorescence detectors, refracted and reflected laser light and luminescence from the flow cell walls is also much higher and will often determine analyte detectability. Especially when flicker noise is present on the background, suppression of these unwanted light contributions may considerably improve the detection limits.

The illuminated volume in a flow cell must be small enough to maintain the chromatographic resolution. It should therefore match the scale of

Table 5
Comparison of two LOD values calculated using the same LC system but different LOD definitions, noise criterions and time constants

Assumptions			
Column	200 × 3.0 mm	Injected concentration	$1.5 \cdot 10^{-8}$ M
Flow-rate	0.5 ml min^{-1}	Analyte signal	90 mV
Analyte retention time	600 s	Rms noise (1 s integration)	2 mV
Injection volume	10 μl	LOD signal-to-noise criterion	S/N = 3
N (plates)	10 000		

Variables	*Experiment A*	*Experiment B*	*Effect on* LOD_A/LOD_B
Detector integration time	0.25 s	4 s	4 ×
Noise definition	peak-to-peak	RMS = 1/5 peak-to-peak	5 ×
LOD definition	injected concentration	peak concentration in cell	12.5 ×
Analyte LOD reported	$1 \cdot 10^{-8}$ *M*	$4 \cdot 10^{-11}$ *M*	250 ×

the separation technique that is used. In Table 6, different liquid-based separation methods and their typical flow cell volumes are listed. For large flow cell compartments, encountered in conventional-size LC, the introduction of the excitation light from a conventional lamp in general will not cause serious problems. In micro-separation techniques, however, it is not possible to focus all lamp excitation light into the detector cell compartment. Laser beams, on the other hand, can easily be adapted to the smallest flow cell diameters.

In most LIF assemblies, flow cell walls are removed from the field of view of the detector or even omitted at all. In Fig. 7 some well-known constructions used in LC–LIF are shown. In the flowing droplet cell, the surface tension forms a solvent bridge between the column outlet and a stainless-steel rod [36]. The development of a micro droplet of 0.4 μl, instead of the original 4 μl, has been reported [37]. Richardson et al. found 10-fold better LODs for a droplet cell compared with a conventional quartz cell using the 351/356 nm output of a Kr-ion laser [38]. A disadvantage of the droplet shape is that the curved surface works as a lens. Furthermore, changes in the eluent composition, for instance during gradient elution, will change the surface tension and, consequently, the shape of the droplet so that the optical alignment of the detector has to be adapted. The amount of refracted and reflected laser light that can reach the detector is reduced by a construction in which the stainless-steel rod is replaced by an optical fiber [39].

In the free falling jet approach of Folestad et al. the effluent from a conventional-size column is forced into a 120 μm internal diameter capillary to increase the linear velocity so that a jet of liquid emerges [40]. The laminar flow could only

Table 6
Typical flow cell volumes used for various separation methods

Separation system	Internal diameter of column (mm)	Typical flow cell volume (μl)
Conventional size LC	4.6/3.0	20
Small-bore LC	1.0	1.0
Packed-capillary LC	0.3	0.05
Open-tubular LC and CE	0.05	< 0.001

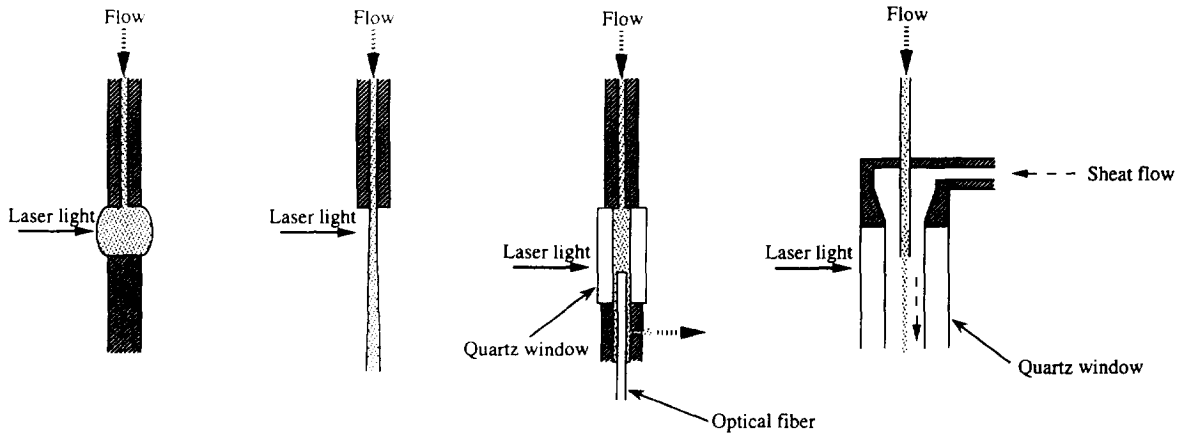

(A) Flowing Droplet (B) Free falling Jet (C) Fiber Flow Cell (D) Sheath Flow Cell

Fig. 7. Flow cell types used for LIF in LC (A–D) and CE (D).

be sustained for relatively high flow-rates (> 1 ml min^{-1}). The same authors extended the applicability range to narrow-bore LC by using smaller capillaries at the column outlet; as a result a flow-rate of 45 μl min^{-1} could be used [41]. As with the flowing droplet, there is much reflected and refracted laser light but this is concentrated in the plane perpendicular to the flow direction. By collecting the fluorescence in an angle of 30° to this plane, scattered light could be decreased by 6 orders of magnitude. The free falling jet and the flowing droplet have been used only sporadically, presumably because of the inconvenience of the open cell construction.

A more practical design which is able to reject reflected and refracted laser light and flow cell wall luminescence by spatially filtering was achieved by Yeung and Sepaniak; here the fluorescence light is collected into a fiber that is put into the bore of the flow cell [42,43]. Transmittance of light through a fiber is only possible for light that enters the fiber within a certain acceptance angle:

$$\sin\theta \leq \frac{\sqrt{n_f^2 - n_c^2}}{n_e} \qquad (19)$$

where θ is the angle between the fiber axis and the light ray and n_f, n_c and n_e are the indices of refraction of the fiber core, fiber cladding and LC eluent, respectively. The fiber-cell assemblies can be adapted to micro-diameter columns by decreasing the sizes of flow cell and optical fiber [44]. Gluckman et al. reported a set-up with a cell volume of 92 nl, which was used for connection to a 250 μm I.D. capillary column [45].

Instead of utilizing the fiber for the collection of light, it can also be used to introduce the excitation light into the flow cell, while collecting the fluorescence light perpendicularly. In this way, the optical path length of the flow cell is increased to illuminate as much analyte inside the cell as is possible without significant loss of chromatographic resolution [21,33,46,47]. Apart from the rejection of unwanted light contributions, optical fibers offer flexibility of the detection system. Furthermore, time discrimination between light signals and the radio frequency noise, which is generated by the fast switching circuits of pulsed lasers and can be picked up by detection systems, is readily achieved. A 25-m fiber was used to cause a time delay of the emission light of about 125 ns, so that the RFI noise is no longer active [48].

When column diameters are very small, fused-silica capillaries are often used as flow cells; they are made transparent by removing a portion of the polyimide coating from the capillary. The flow cell usually is part of the separation column as coupling connections will destroy the chro-

matographic resolution [49,50]. The stray light contribution from capillaries often is so high that spatial filtering by means of microscope objectives is used and collecting optics are positioned out of the horizontal plane formed by the laser beam and the direction of the capillary [51,52]. Stray light intensity can be considerably decreased by immersing the capillary in an index-matching fluid having nearly the same refraction index as fused silica [53].

Detection volumes in the sub-nl range are achieved with the sheath-flow cell cuvette [54,55] and have been applied in "single-molecule" detection [21,56–58]. In this approach the column effluent is ensheathed by another flowing stream of similar refractive index. Under laminar flow conditions, the integrity of the small sample stream diameter is maintained. As the cuvette walls are far removed from the sample stream, flow cell wall luminescence and scattered stray light can easily be removed by spatial filtering. The cell can be incorporated in the electrical circuit of a capillary electrophoresis (CE) separation system, using an ensheating buffer stream.

3.3. Comparison between conventional fluorescence and LIF detectors

Applying LIF detection in LC is only useful when the analyte detectability obtained with conventional fluorescence detectors can be improved. For miniaturized systems, the light output of conventional sources can not be fully exploited because only a small part of the available excitation light can be directed into the flow cell. Recently, a filter fluorimeter has been described by Dovichi and co-workers which consists of a 75-W xenon-arc lamp and an efficient optical system; the excitation set-up was capable of delivering microwatts of optical power within a 10-nm spectral bandwidth and concentrated to a spot of about 180 mm in diameter [59]. On this scale (flow cell diameters typically are 50 μm), the spatial coherence of lasers is essential and LIF offers detection limits that are often more than three decades better than in conventional fluorimetry [60]. On the other hand, in conventional-size LC the introduction of light from a lamp into a flow cell diameter of 1 mm, generally will not be a problem. Then, the difference between LIF and conventional fluorimetry will be determined by four factors. A brief discussion, which partly repeats statements made earlier in this paper, is as follows.

3.3.1. The matching of the absorption spectrum of the analyte under study with the available laser line

Contrary to laser excitation sources, conventional fluorimeters equipped with a xenon-arc lamp and excitation monochromator, can be tuned readily to the absorption maximum of the analyte of interest. At first sight one might suspect that the lack of optimum excitation due to the limited tunability of the excitation source, as is the case with most lasers, can be counterbalanced by increasing the light power. However, the background signal also depends linearly on the excitation power. Consequently, even under shot-noise conditions, the gain in analyte detectability increases only with the square root of the incident radiation whereas it is directly proportional with the molar absorption coefficient. When flicker noise is dominant, increasing the laser power has no positive effect at all; tuning at a more favourable absorption wavelength is the only way to improve the detection limits. The influence of wavelength selection is clearly illustrated in Fig. 8, derived from a recent paper of Zare and co-workers [61]. In this figure, the electropherograms of phenanthrene obtained with near-UV excitation at 325 nm and deep-UV excitation at 257 nm are compared. In both situations the laser power at the capillary is 10 mW. Considering the 20-fold concentration difference, the improvement in sensitivity obtained by applying deep-UV excitation is remarkable.

3.3.2. The amount of radiation that can be introduced into the flow cell

For commercially available detectors equipped with a xenon-arc lamp and monochromator, the average output that reaches the flow cell compartment is limited to about 100 μW. In LIF detection a laser output of 1 W is about the maximum that can be used before saturation

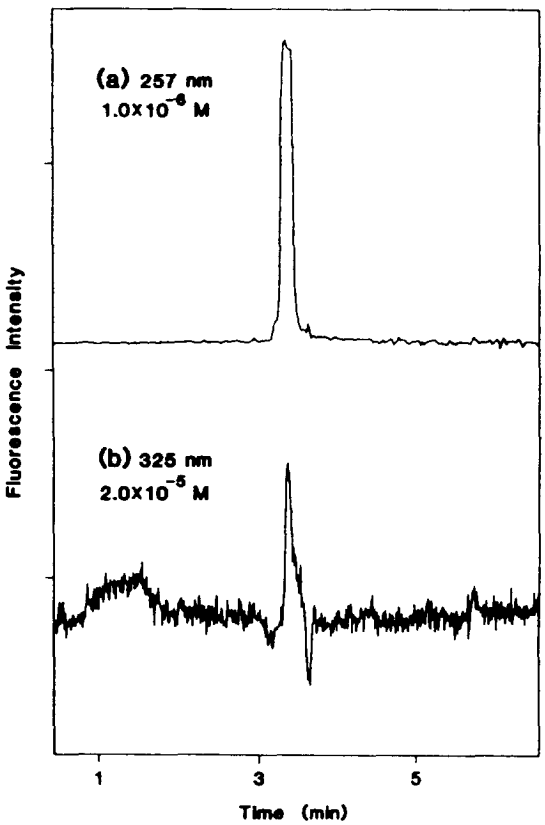

Fig. 8. Comparison of detection sensitivity for phenanthrene between near-UV and deep-UV laser excitations. (a) Electropherogram of $1.0 \cdot 10^{-6}$ *M* phenanthrene with deep-UV-LIF detection: laser wavelength 257 nm; laser power 10 mW; injection volume 0.5 nl. (b) Electropherogram of $2.0 \cdot 10^{-5}$ *M* phenanthrene with near-UV-LIF detection; laser wavelength 325 nm; laser power 10 mW; injection volume 0.5 nl. Note the 20-fold concentration difference. From Ref. [61].

occurs. This would imply that on the basis of excitation power only, the LODs measured with LIF will be two orders of magnitude better provided that shot-noise conditions are realized.

3.3.3. The stability of the output of the light source, especially important at high backgrounds

Whereas conventional light sources provide stable outputs, lasers are inherently less stabile and fluctuations on the order of 1–2% are not unusual for CW lasers; in other words, in various practical situations flicker noise dominates if no special measures are taken. For pulsed lasers, the pulse-to-pulse stability is even worse: deviations can be as large as 50% so that signal averaging over a substantial number of pulses is required to decrease the noise to acceptable levels.

3.3.4. The ability to measure in a window of the eluent Raman spectrum

If lasers are used, the Raman spectrum is highly resolved (see Fig. 3) and the analyte fluorescence can be detected in the spectral regions between the lines. As the Raman lines are at least as broad as the excitation band it is almost impossible for conventional fluorimeters with a typical 10–20 nm spectral band-pass to reject the Raman light completely. If the monochromators of the fluorimeter are equipped with a grating, the excitation and emission bandwidths expressed in wavelengths, are nearly constant over the whole spectrum. The possibility of measuring analyte fluorescence in a "Raman gap" is therefore optimal in the red part of the spectrum. To prevent the detection of excitation light transmitted by the grating in the second-order diffraction mode and stray radiation of wavelengths not selected by the monochromators, optical filters should be used in addition.

Only few authors have extensively compared their LIF results with data obtained using a conventional fluorescence detector under the same chromatographic conditions. In Table 7 literature data are assembled in which LODs obtained with LIF and conventional fluorimetry are compared. In all but one case, LIF yields better results; the average gain is 10–100 fold. The maximum (6000) and minimum (0.3) gain reported for fluorescein isothiocyanate and 9-methylanthracene can be interpreted using the arguments presented above. The absorption spectrum of fluorescein isothiocyanate has a perfect match with the high-power 488-nm line of the argon-ion laser. As the background due to luminescent impurities is relatively low upon excitation with visible light, shot noise is dominant which means that the available power can be fully exploited. On the other hand, under the

Table 7
Comparison of analyte detectability in LC using laser-induced (LIF) and conventional fluorescence (CF) detection

Analyte	LOD_{CF}/LOD_{LIF}	LIF system			
		Laser	λ_{ex} (nm)	Power (mW)	Ref.
Dansyl-analine	10	Ar-ion	351–364	0.85	70
OPA-amino acids[a,c]	45	Ar-ion	334–364	250	44
NDA-amino acids[b,c]	78	Ar-ion	458	900	44
Coumarin 7	6	HeCd	442	13	33
Benzo[*a*]pyrene	10	N_2/BBQ	386	15	69
NDA-amino acids	31	N_2/coumarin 1	454	2.4	39
9-Methylanthracene	0.15	HeCd	325	0.3	52
Adriamycin	30	Ar-ion	488	8	26
9-Hydroxymethylanthracene	250	Ar-ion	351–364	200	62
Fluorescein isothiocyanate	6000	Ar-ion	488	2000	62
Benzo[*a*]pyrene	5	Ar-ion	257	5	65

[a] OPA, *o*-phthalaldehyde.
[b] NDA, 2,3-naphthalenedialdehyde.
[c] Precolumn derivatisation at high analyte concentration, with subsequent dilution prior to injection.

experimental conditions applied in Ref. [52], 9-methylanthracene strongly absorbs the 365-nm line of a mercury arc lamp, while the 325-nm HeCd laser line is only weakly absorbed. Furthermore, the background encountered in UV-LIF is relatively high so that in combination with the unstable HeCd laser, flicker noise is the (undesired) limiting factor.

It should be emphasized that the data in Table 7 refer to the analysis of standard solutions. When analysing real samples by means of LC with LIF detection, the presence of interfering compounds usually determines the much higher detection limits that can be achieved. In such a situation, the gain that can be obtained by using LIF instead of conventional fluorescence detection is small when conventional-size LC is utilized and flicker noise dominates. The large gap existing between the ideal "standard" situation and real trace-level analysis is further discussed in the next section.

3.4. Applications

Although the number of compounds that exhibit native fluorescence is rather limited, there are highly interesting analytes within that group, such as, e.g., polynuclear aromatic hydrocarbons (PAHs) and their metabolites, aflatoxins, aromatic amino acids, and several vitamins and drugs such as alkaloids and steroids [1]. Unfortunately, most of these compounds require excitation with UV light, a part of the spectrum that is not easily covered by lasers, although major developments are taking place in this area today. This is also the reason why, since the introduction of LIF detection in LC, much attention has been devoted to the use of chemical derivatization procedures involving the reaction of the analyte with a strongly fluorescent label that can be excited by visible laser light (naphthalene-2,3-dialdehyde [44], fluorescein isothiocyanate [55,62]). Extremely low LODs have been reported in the literature, such as a value of 1.2 pM (injected concentration, $S/N_{peak} = 3$) for phenylalanine derivatized with fluorescein isothiocyanate [62]. However, such LODs generally do not reflect "real-life" situations because they are based on the analysis of standard solutions prepared by derivatizing the test analytes at high concentrations, with subsequent dilution prior to injection (cf. Table 7). In actual practice, when low analyte concentrations have to be determined, it is not exceptional to use a 10 000-fold excess of label, and improving analyte detectability often turns out to

be limited by the (slow) kinetics of the labelling reaction. Impurities that are present in the labelling reagent (even in very low amounts) and the formation of side-products, also adversely affect the final result [63]. This has been discussed in some detail by Kwakman et al. [5] for chemiluminescence detection in LC. It has also been emphasized by Mank et al. who have recently described a covalent labelling of thiols appropriate to utilize visible diode laser induced fluorescence detection [64]. Since the present review deals only with native-fluorescent analytes, such problems, of course, do not play any role at all.

Table 8 summarizes literature data on LC with LIF detection for some native-fluorescent analytes. All data apply for standard solutions, except the measurements of adriamycin, which were carried out in urine. In most studies attention has been paid to the determination of PAHs which can be excited by the shortest wavelengths of the argon-ion-, krypton-ion-, HeCd- and N_2 laser.

The data reported by different workers can not be compared directly because of differences in the experimental conditions (analytes, separation systems, lasers). Table 8 should therefore merely be used to extract some general conclusions on LIF detection in [conventional-size, micro and open-tubular (OT)] LC and CE.

(i) In general, the lowest concentration detection limits are found in conventional-size LC, where the optical path lengths are large and optically favourable flow cell assemblies can be used. Although the absolute detection limits in packed capillary and open tubular LC are extremely low, they require the injection of rather concentrated sample solutions.

(ii) Despite the fact that the light power of diode lasers is relatively low, analyte detectability often is very good. With the long excitation wavelengths used, the background is caused almost completely by Raman scatter, even though it is considerably less intense in the red part of the spectrum due to its λ^{-4} dependence. Furthermore, the light output of diode lasers is very stable so that the background contains only shot noise. Diode laser induced fluorescence (DIO-LIF) has shown to have interesting possibilities for the detection of photosensitizers in photodynamic therapy [29]. A well-known example is disulfonated aluminum phthalocyanine $AlPcS_2$ (see Fig. 9b), which comprises up to sixteen isomeric compounds. Applying DIO-LIF at 670 nm (power 10 mW), for the major component in the liquid chromatograms of spiked urine and faeces extracts, a detection limit of $7 \cdot 10^{-12}$ M could be obtained (20 times lower than achievable with a conventional fluorescence detector). This sensitivity is high enough to obtain detailed information about the excretion of the various isomers: Fig. 9a shows chromatograms of urine samples over 30 days after injection of the rat with 1 μmol/kg $AlPcS_2$. Evidently, such detailed information is highly relevant from a pharmacokinetic point of view.

In the green part of the spectrum impurity fluorescence is still relatively weak and high-laser powers can be applied [26,42]. An interesting example of LIF detection of a natively fluorescent analyte is the bioanalysis of the cytostatic drug doxorubicin (adriamycin) in human plasma [26], see Fig. 10. This compound can be appropriately excited with the 488 nm line of the Argon-ion laser; its emission maximum is at 595 nm. For sample clean-up, only a one-step protein precipitation was needed. Compared to conventional fluorescence detection the determination limit (200 pg/ml) was improved more than one order of magnitude even by using an air-cooled Argon-ion laser providing 8 mW at 488 nm. Presumably an additional gain of at least one decade will be obtained by applying a high-power laser giving about 1 W, but the low-power system suffices for the problem at hand.

(iii) When excitation is performed with UV light, the instability of the laser light source is a serious disadvantage. For the relatively unstable HeCd laser, a stabilizing circuit or a ratioing technique was used to suppress the amount of flicker noise [36,45,33,52]. The LODs measured with deep-UV LIF were all limited by the combination of high backgrounds and fluctuations in the laser output [61,65–68]. In these studies, only part of the available laser power was used.

Table 8
Detectability of native-fluorescent analytes using LC-LIF and CE-LIF

Analyte	Excitation			Separation system			LOD			Time constant (s)	Ref.
	Laser	λ_{ex} (nm)[a]	Power (mW)[a]	Column diameter (m-m)	Cell type	Optical path length (mm)	Injected concentration	Detector concentration	Injected mass		
Aluminium phthalocyanine	Diode	670	10	3.1	em fiber[b]	1.1	7 p*M*	480 f*M*	130 fg	0.5	29
Adriamycin	Ar-ion	488	1200	4.6	em fiber	1.0	n.i.a.[c]	19 p*M*	10 pg	2	43
Adriamycin	Ar-ion	488	1000	3.0	square quartz	1.5	140 p*M*	230 p*M*	8 pg	1	26
Coumarin 7	HeCd	442	13	4.6	ex fiber[d]	5	3 p*M*	n.i.a.	11 fg	0.2	33
Fluoranthene	N_2/PBD	366	2.5	CS[e]	droplet	2	3.7 n*M*	340 p*M*	15 pg	3	38
Fluoranthene	Kr-ion	351 + 356	1500	4.6	free-falling jet	0.12	3 p*M*	80 f*M*	6 fg	n.s.[f]	40
Fluoranthene	Kr-ion	351 + 356	200	CS	droplet	2	3.7 n*M*	340 p*M*	15 pg	3	38
Benzo[*a*]pyrene	N_2/BBQ	386	15	4.0	quartz	n.s.	90 p*M*	10 p*M*	1.1 pg	4	69
Aflatoxin B_{2a}	HeCd	325	8	CS	droplet	2	375 p*M*	9 p*M*	1.1 pg	3	36
Anthracene	XeCl	308	20	4.6	droplet	2	225 n*M*	11 n*M*	800 pg	n.s.	71
Benzo[*a*]pyrene	Ar-ion	257	5	3.0	em fiber	1.1	200 p*M*	9 p*M*	500 fg	1	65
Pyrene	HeCd	325	6.5	0.25 capillary	em fiber	0.050	3 n*M*	n.i.a.	120 fg	0.3	45
Perylene	N_2/BBQ	386	1	0.35 capillary	capillary	n.s.	60 n*M*	n.i.a.	850 fg	n.s.	72
Riboflavin	HeCd	442	4.1	0.025 OTLC	on-column	0.025	n.i.a.	4.8 n*M*	175 fg	1	52
Fluoranthene	HeCd	325	1.2	0.025 OTLC	on-column	0.025	500 n*M*	6 n*M*	100 fg	1	49
Conalbumin	Ar-ion	275	n.s.	0.050 CE	on-column	0.050	300 p*M*	n.i.a.	n.i.a.	n.s.	67
Tryptophan							5 n*M*	n.i.a.	n.i.a.	n.s.	67
Conalbumin	Ar-ion	257	9	0.050 CE	on-column	0.050	30 n*M*	n.i.a.	n.i.a.	n.s.	66
2-Methylanthracene	Ar-ion	257	10	0.025 CE	on-column	0.025	300 p*M*	n.i.a.	30 ag	n.s.	61
Tryptophan	KrF	248	12	0.075 CE	on-column	0.075	5 n*M*	n.i.a.	n.i.a.	0.05	68

Limits of detection from originally reported data were recalculated for S/N = 3 criterion (peak-to-peak noise). If neccessary, LOD detector concentrations (cf. CD_{det} in Eq. 8) were calculated from chromatogram figures

[a] For pulsed laser the average power is used.

[b] Emission light collected with fiber.

[c] No information available for recalculation.

[d] Excitation light coupled in via fiber.

[e] Conventional size, no information on exact column diameter available.

[f] Not stated in paper.

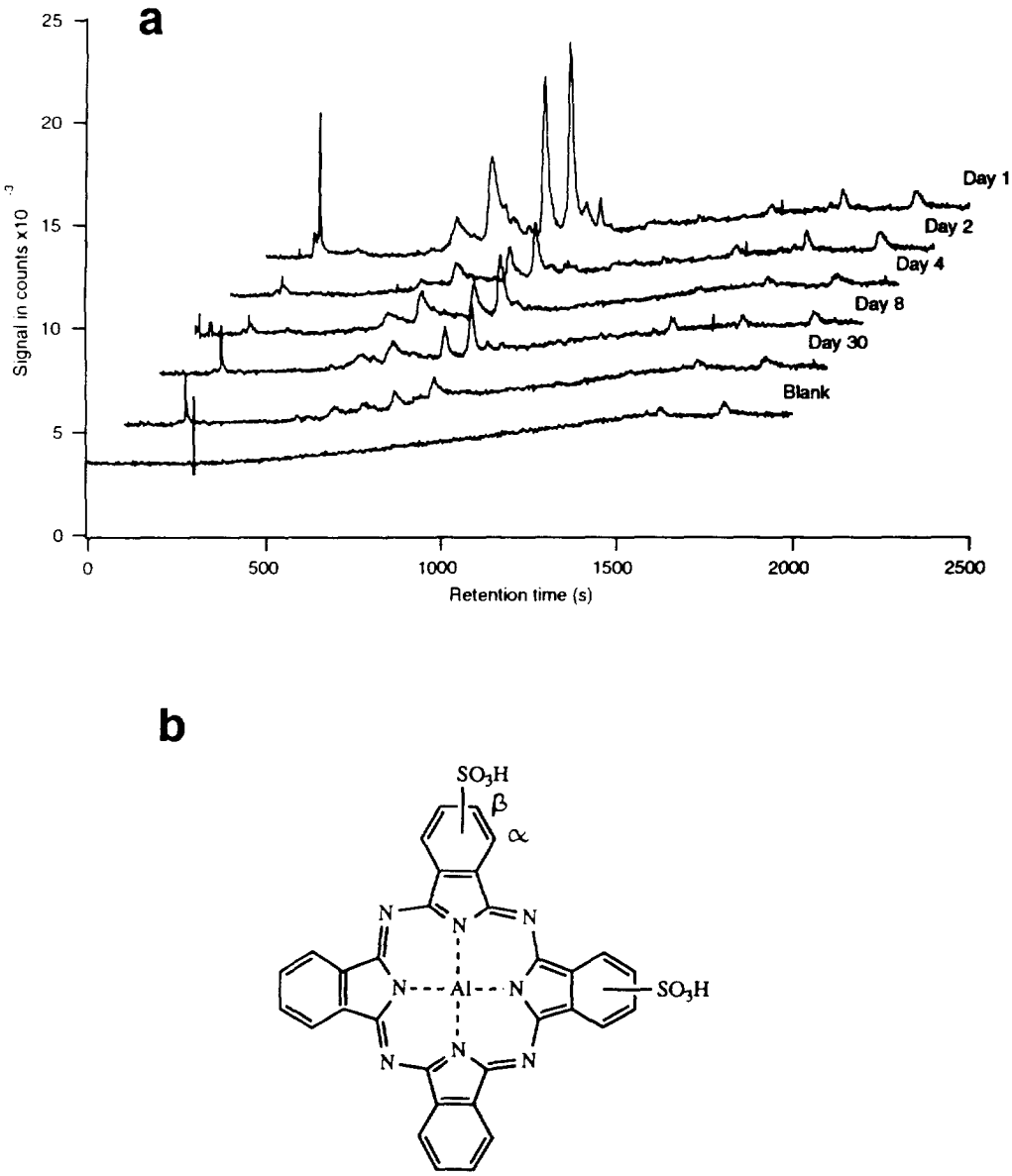

Fig. 9. (a) Chromatograms (performing linear gradient elution methanol–phosphate buffer, pH 5.0, from 25:75 to 90:10, v/v) of extracted urine samples after injection with 1 μmol/kg $AlPcS_2$; from Ref. [29]. (b) Structure of $AlPcS_2$.

(iv) As regards pulsed lasers it is remarkable that good LODs have been reported despite the well-known pulse-to-pulse instability [68,69]. Obviously, time discrimination is highly effective in decreasing background signals while pulse averaging diminishes the flicker noise.

(v) The LIF systems used for detection in CE demonstrate the potential of the new excitation possibilities in the deep-UV. Before the introduction of these laser lines, the analytes studied in the quoted work had to be determined using chemical derivatization of the amino group with subsequent analysis.

Deep-UV lines are not only useful for the

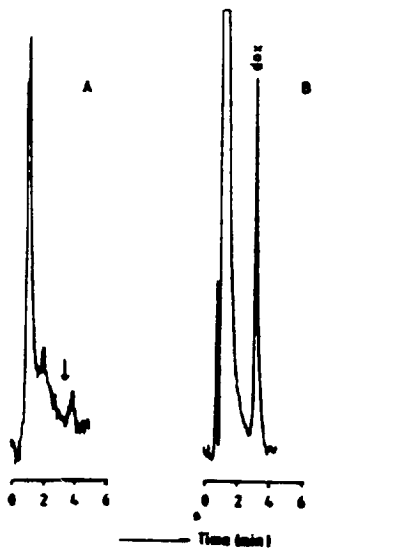

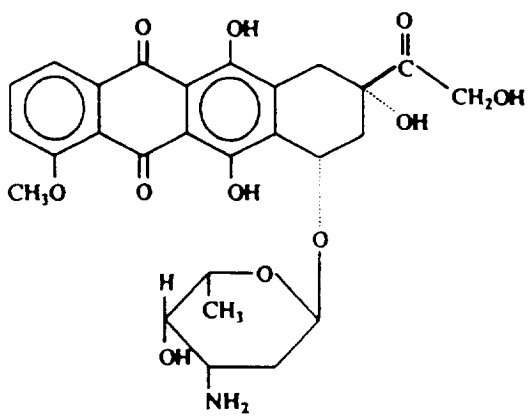

Fig. 10. Analysis of plasma samples pretreated by one-step protein precipitation. LIF detection was performed with an air-cooled Argon-ion laser (488 nm, 8 mW). The chromatograms were obtained using a conventional size RP-18 column; the mobile phase was a mixture of aqueous orthophosphoric acid solution (0.01 *M*) and acetonitrile (3:1, v/v). (A) Blank plasma sample; (B) plasma sample spiked with 4 ng/ml doxorubucin; (c) shows the chemical structure of doxorubicin (adriamycin). From Ref. [26].

detection of analytes which can not be excited by visible light. Since, at present, wavelength tuning of lasers over a large spectral range is not possible, the application range of a LIF system is determined by the coincidental match of the absorption spectrum of a particular analyte and the laser line. Because most analytes exhibit relatively high molar absorptivities at wavelengths shorter than 300 nm, a LIF detector operating in the deep-UV region has more potential than longer-wavelength systems. On the other hand its selectivity will be distinctly less, and the performance of such systems in real-life situations still has to meet the test.

4. Conclusions and future developments

The present review shows that LIF application in LC is not simply a matter of replacing a conventional light bulb, but that it involves adapting flow cells, optics, and detector instrumentation. Compared with laser excitation in the visible region, the problems encountered in deep-UV LIF are essentially different. In practice, background due to Raman scatter of the LC eluent can be readily excluded; on the wavelength scale it is so close to the laser line that it does not interfere with the analyte fluorescence and can be fully rejected by a simple cut-off filter. However, background luminescence from the flow cell assembly and impurities in the LC system show up strongly upon UV exposure. Eluents should therefore be purified and high-quality optical components should be used. As a result of the high background signal and instabilities in the laser output, flicker noise is already dominant at low excitation power. Under these conditions, the limit of detection can not be further improved because the noise amplitude and sample signal are both directly proportional with the laser power; the use of ratioing techniques and laser output stabilizers is of crucial importance.

As regards future developments, several new types of laser systems are now being developed. For detection of native-fluorescent analytes, the main interest will be on lasers which provide deep-UV light. An argon-ion laser producing these deep-UV lines already has been commercialized and hundreds of milliwatts are available.

Unfortunately, such a system is both expensive and large and requires high-power electrical facilities and extensive water cooling. The development of two other types of lasers seems more promising. Small-size excimer lasers are available today which operate on KrF gas and produce 248-nm light pulses at a frequency of 2000 Hz. Such a high repetition frequency enables efficient reduction of the noise caused by peak-to-peak fluctuations, by utilizing pulse averaging. Secondly, the use of diode lasers as pump source for neodymium lasers combined with a high-performance wavelength convertor has opened the way for an air-cooled and compact version that provides 266-nm light with low optical noise.

The above laser systems deliver only fixed wavelengths. For optimum excitation, tunability over a large spectral range is desirable. In this context, new developments in optical parametric oscillators (OPOs) combined with frequency mixing are interesting [7]. An OPO system, which is a tunable frequency converter based on an Nd:YAG laser, offers a "flat" spectral tuning curve in the deep UV. Although OPOs are still in the experimental stage, they bring us a step closer to the dream of every (analytical) spectroscopist: a versatile laser system providing tunable radiation from the visible region to the deep-UV.

References

[1] N. Ichinose, G. Schwedt, F.M. Schnepel and K. Adachi, in J.D. Winefordner (Editor), *Fluorimetric Analysis in Biomedical Chemistry*, Wiley, New York, 1991, Chs. 4 and 5.

[2] W.G.R. Bayens, D. de Keukeleire and K. Kordikis (Editors), *Luminescence Techniques in Chemical and Biomedical Analysis*, Marcel Dekker, New York, 1991.

[3] J.W. Hofstraat, C. Gooijer and N.H. Velthorst, in S.G. Schulman (Editor), *Molecular Luminescence Spectroscopy*, Part 3, Wiley, New York, Ch. 9, 1993.

[4] C.M.B. van den Beld and H. Lingeman, in W.G.R. Bayens, D. de Keukeleire and K. Korkidis (Editors), *Luminescence Techniques in Chemical and Biomedical Analysis*, Marcel Dekker, New York, 1991, Ch. 9.

[5] P.J.M. Kwakman, H. Koelewijn, I. Kool, U.A.Th. Brinkman and G.J. de Jong, *J. Chromatogr.*, 511 (1990) 155.

[6] T.H. Maiman, *Nature*, 187 (1960) 493.

[7] J.J. Ewing, *Laser Focus World*, November 1993, p. 105.

[8] J. Hecht, *Laser Focus World*, May 1992 p. 105, December 1992 p. 97, August 1993 p. 67.

[9] J. Hecht, *Laser Focus World*, April 1992 p. 77, June 1992 p. 63, May 1993 p. 87.

[10] J. Hecht, *The Laser Guidebook*, McGraw-Hill, New York, 2nd ed., 1992.

[11] J. Fabian, H. Nakazumi and M. Matsuoka, *Chem. Rev.*, 92 (1992) 1197.

[12] A.J.G. Mank, H. Lingeman and C. Gooijer, *Trends Anal. Chem.*, 11 (1992) 210.

[13] G. Patonay and M.D. Antoine, *Anal.Chem.*, 63 (1991) 321A.

[14] I. Imasaka, A. Tsukemoto and N. Ishibashi, *Anal. Chem.*, 61 (1989) 2285.

[15] R. Niessner, U. Panne and H. Schröder, *Anal. Chim. Acta*, 255 (1991) 231.

[16] S.H. Wu and N.J. Dovichi, *J. Chromatogr.*, 480 (1989) 141.

[17] S.A. Asher, R.W. Bormett, X.G. Chen, D.H. Lemmon, N. Cho, P. Peterson, M. Arrigoni, L. Spinelli and J. Cannon, *Appl. Spectrosc.*, 47 (1993) 628.

[18] P.A. Harmon, J. Teraoka and S.A. Asher, *J. Am. Chem. Soc.*, 122 (1990) 8789.

[19] I. Carmichael and G.L. Hug, *J. Phys. Chem.*, 89 (1985) 4036.

[20] R.R. Birge, in D.S. Kliger (Editor), *Ultrasensitive Laser Spectroscopy*, Academic Press, New York, 1983, Ch. 2.

[21] R.A. Mathies, K. Peck and L. Stryer, *Anal. Chem.*, 62 (1990) 1766.

[22] D.C. Nguyen, R.A. Keller, J.H. Jett and J.C. Martin, *Anal. Chem.*, 59 (1987) 2158.

[23] A.P. Larson, H. Ahlberg and S. Folestad, *Appl. Opt.*, 32 (1993) 794.

[24] A. Taylor and E.S. Yeung, *Anal. Chem.*, 64 (1992) 1741.

[25] J.H. Sugarman and R.K. Prud'homme, *Ind. Eng. Chem. Res.*, 26 (1987) 1449.

[26] C.M.B. van den Beld, *Ph.D. Thesis*, Leiden University, The Netherlands, 1991.

[27] T.G. Matthews and F.E. Lytle, *Anal. Chem.*, 51 (1979) 583.

[28] T.G. Matthews and F.E. Lytle, *Anal. Chem.*, 51 (1979) 583.

[29] A.J.G. Mank, C. Gooijer, H. Lingeman, N.H. Velthorst and U.A.Th. Brinkman, *Anal. Chim. Acta.*, 290 (1994) 103.

[30] R.J. van de Nesse, G.Ph. Hoornweg, C. Gooijer, U.A.Th. Brinkman, N.H. Velthorst and B. Law, *Anal. Chim. Acta*, 281 (1993) 373.

[31] J.E. Knoll, *J. Chromatogr. Sci.*, 23 (1985) 422.

[32] J.D. Ingle, Jr. and S.R. Crouch, *Spectrochemical Analysis*, Prentice-Hall, Englewood Cliffs, NJ, 1988, Ch. 5.

[33] J.M. Bostick, J.W. Strojek, T. Metcalf and T. Kuwana, *Appl. Spectrosc.*, 46 (1991) 1532.

[34] J.P. Foley and J.G. Dorsey, *Chromatographia*, 18 (1984) 503.

[35] ACS Committee on Environmental Improvement, *Anal. Chem.*, 52 (1980) 2242.
[36] G.J. Diebold and R.N. Zare, *Science*, 196 (1977) 1439.
[37] K.H. Milby and R.N. Zare, *Int. Lab.*, March/April (1984) 10.
[38] J.H. Richardson, K.M. Larson, G.R. Haugen, D.C. Johnson and J.E. Clarkson, *Anal. Chim. Acta*, 116 (1980) 407.
[39] K.-I. Tsunoda, A. Nomura, J. Yamada and S. Nishi, *Anal. Chim. Acta*, 229 (1990) 3.
[40] S. Folestad, L. Johnson, B. Josefsson and B. Galle, *Anal. Chem.*, 54 (1982) 925.
[41] S. Folestad, B. Galle and B. Josefsson, *J. Chromatogr. Sci.*, 23 (1985) 273.
[42] E.S. Yeung and M.J. Sepaniak, *Anal Chem.*, 52 (1980) 1465A.
[43] M.J. Sepaniak and E.S. Yeung, *J. Chromatogr.*, 190 (1980) 377.
[44] M.C. Roach and M.D. Harmony, *Anal. Chem.*, 59 (1987) 411.
[45] J. Gluckman, D. Shelly and M. Novotny, *J. Chromatogr.* 317 (1984) 443.
[46] H. Todiriki and A.Y. Hirakawa, *Chem. Pharm. Bull.*, 32 (1984) 193.
[47] S.A. Soper, S.M. Lunte and T. Kuwana, *Anal. Sci.*, 5 (1989) 23.
[48] K.-I. Tsunoda, A. Nomura, J. Yamada and S. Nishi, *Anal. Chim. Acta*, 229 (1990) 3.
[49] H.P.M. van Vliet and H. Poppe, *J. Chromatogr.*, 346 (1985) 149.
[50] M. Verzele and C. Dewaele, *J. High Resolut. Chromatogr. Chromatogr. Commun.*, 10 (1987) 248.
[51] K.J. Miller and F.E. Lytle, *J. Chromatogr.*, 648 (1993) 245.
[52] E.J. Guthrie, J.W. Jorgenson and P.R. Dluzneski, *J. Chromatogr. Sci.*, 22 (1984) 171.
[53] Y. Kurosu, T. Sasaki and M. Saito, *J. High Resolut. Chromatogr.*, 14 (1991) 186.
[54] L.W. Hersberger, J.B. Callis and G.D. Christian, *Anal. Chem.*, 51 (1979) 1444.
[55] Y.F. Cheng and N.J. Dovichi, *Science*, 242 (1988) 562.
[56] D.C. Nguyen, R.A. Keller, J.H. Jett and J.C. Martin, *Anal. Chem.*, 59 (1987) 2158.
[57] N.J. Dovichi, J.C. Martin, J.H. Jett, M. Trkula and R.A. Keller, *Anal. Chem.*, 56 (1984) 348.
[58] J.H. Hahn, S.A. Soper, H.L. Nutter, J.C. Martin, J.H. Jett and R.A. Keller, *Appl. Spectrosc.*, 45 (1991) 743.
[59] E. Arriaga, D.Y. Chen, X.L. Cheng and N.J. Dovichi, *J. Chromatogr. A*, 652 (1993) 347.
[60] M. Albin, R. Weinberger, E. Sapp and S. Moring, *Anal. Chem.*, 63 (1991) 417.
[61] S. Nie, R. Dadoo and R.N. Zare, *Anal. Chem.*, 65 (1993) 3571.
[62] C.M.B. van den Beld, H. Lingeman, G.J. van Ringen, U.R. Tjaden and J. van der Greef, *Anal. Chim. Acta*, 205 (1988) 15.
[63] C.M.B. van den Beld, U.R. Tjaden, N.J. Reinhoud, D.S. Stegehuis and J. van der Greef, *J. Control. Rel.*, 13 (1990) 129.
[64] A.J.G. Mank, E.J. Molenaar, H. Lingeman, C. Gooijer, U.A.Th. Brinkman and N.H. Velthorst, *Anal. Chem.*, 65 (1993) 2197.
[65] R.J. van de Nesse, G.Ph. Hoornweg, C. Gooijer, U.A.Th. Brinkman and N.H. Velthorst, *Anal. Chim. Acta*, 227 (1989) 173.
[66] D.F. Swaile and M.J. Sepaniak, *J. Liq. Chromatogr.*, 14 (1991) 869.
[67] T.T. Lee and E.S. Yeung, *J. Chromatogr.*, 595 (1992) 319.
[68] K.C. Chan, G.M. Janini, G.M. Muschik and H.J. Issaq, *J. Liq. Chromatogr.*, 6 (1993) 1877.
[69] N. Furuta and A. Otsuki, *Anal. Chem.*, 55 (1983) 2407.